J. exp. Biol. **157**, 391–408 (1991)
Printed in Great Britain © *The Company of Biologists Limited 1991*

TEMPORAL ANALYSIS OF SNAIL FEEDING RHYTHMS: A THREE-PHASE RELAXATION OSCILLATOR

BY C. J. H. ELLIOTT AND T. ANDREW*

Department of Biology, University of York, Heslington, York, YO1 5DD, UK

Accepted 17 January 1991

Summary

1. Rhythmic fictive feeding was recorded from the motoneurones of the buccal ganglia of *Lymnaea stagnalis*. The times of the action potentials were recorded by microcomputer and the lengths of the three phases (N1, N2 and N3) making up each feeding cycle were determined.

2. During spontaneous rhythmic fictive feeding in *Lymnaea stagnalis* the cycle period varied randomly.

3. Most of the variation in cycle period arose from alterations in the duration of the N3 (swallowing) phase of the rhythm; the N1 (protraction) and N2 (rasp) phases were fixed in length.

4. The firing rates of feeding motoneurones active in the N1 and N3 phases increased with feeding rate: this was not true of those active in the N2 phase.

5. In rhythms produced by stimulating the SO modulatory interneurone, both the N1 and N3 phases varied in duration. The N2 duration remained constant.

6. The temporal analysis is accounted for by the neuronal model based on the synaptic interactions recorded by Elliott and Benjamin (1985*a*,*b*; *J. Neurophysiol.* **54**, 1396–1421).

Introduction

The feeding system of gastropod molluscs has provided many insights into the neural basis of behaviour, including the sensory control of behaviour, the mechanisms of pattern generation and neuromodulation. One of the best described systems is that of the pond snail *Lymnaea stagnalis* (for a review, see Benjamin and Elliott, 1989). In the process of trying to build a satisfactory model of the feeding behaviour, the *sequence* of neural activity has been extensively studied. In this paper, our aim is to extend the analysis and begin to account for the *timing* of neural activity in the *Lymnaea* feeding system.

The pond snail feeds by rhythmic protraction and retraction of the radula, with each cycle taking 3–5 s. Cycles of activity may follow one another immediately, or be separated by quiescent periods, with the feeding rate dependent upon the sugar

* Present address: The Institute of Psychiatry, 101 Denmark Hill, London SE5 8AF.

Key words: mollusc, feeding, rhythms, *Lymnaea stagnalis*.

concentration or abundance of algae (Dawkins, 1974; Kemenes *et al.* 1986). Recordings from semi-intact preparations show that the rhythmic movement is produced by coordinated activity in the muscles of the buccal mass and that each cycle consists of three successive movements: protraction of the radula, rasping and swallowing (Rose and Benjamin, 1979). These recordings also show that the three movements reflect three phases of activity in the buccal motoneurones (cell types 1–10).

In the isolated central nervous system (CNS), the same three-phase rhythm of 'fictive feeding' is still present in many preparations (Benjamin and Rose, 1979; Rose and Benjamin, 1981*a*,*b*). Recordings from the isolated CNS show that the feeding rhythm can be accounted for on the basis of synaptic inputs to the motoneurones from just three kinds of multi-action interneurone. These three kinds of interneurone have been identified morphologically and physiologically and are called N1, N2 and N3. Each type of interneurone is only active in one phase of the feeding cycle, with the N1 activity corresponding to protraction, the N2 activity to rasping and the N3 cells firing during swallowing (Rose and Benjamin, 1981*b*).

The success of the neuroethological approach in analysing the sequence of *Lymnaea* feeding behaviour was extended by the characterisation of the N1, N2 and N3 interneurones. Each kind of N-cell can reset the phase of the rhythm, showing that all these cells are part of the pattern-generating network. Furthermore, their synaptic connections and endogenous membrane properties can account for the normal N1→N2→N3→N1... sequence of activity (Elliott and Benjamin, 1985*a*, for further details see the Discussion). However, it seems that the timing of the rhythm is determined not by the short-latency, fast-acting synaptic potentials recorded between the identified premotor interneurones (N1, N2 and N3 cells) but by the endogenous properties of the cells themselves, for although the duration of each of the phases of activity is at least 1 s, all the synaptic potentials lasted for less than 100 ms. The membrane properties that evidently control the timing include the abilities to burst endogenously (N1 interneurones), to form plateau potentials (N2 cells) and to show post-inhibitory rebound (N3 interneurones) (Elliott and Benjamin, 1985*a*).

To analyse the importance of the contributions made by the different kinds of membrane properties to the timing of the feeding rhythm, we need to know the temporal pattern of the fictive feeding rhythm. The purpose of this paper is to describe quantitatively the alterations in neural pattern that occur when the rate of the feeding rhythm changes. Such changes may occur spontaneously or as a result of stimulating modulatory interneurones.

The identified modulatory interneurones include the SO (slow oscillator) cell (a single cell located in the buccal ganglia, Rose and Benjamin, 1981*a*; Elliott and Benjamin, 1985*b*) and the cerebral giant cells (CGCs, McCrohan and Benjamin, 1980; Tuersley and McCrohan, 1988; Benjamin and Elliott, 1989). In the isolated CNS, the SO is usually silent, even when fictive feeding is occurring in the rest of the network. Activating the SO increases the feeding rate or, if the preparation is

dormant, SO activity will start up cycles of the feeding pattern (Rose and Benjamin, 1981*a*). The effects of the SO are principally mediated by connections with the N1 and N2 interneurones. The other modulatory interneurones considered here are the CGCs, which fire tonically in the isolated CNS, at between 0.5 and 2 Hz. These make connections with the motoneurones, the N-cells and the SO and can accelerate or inhibit the feeding rate depending on the previous state of the feeding system (McCrohan and Audesirk, 1987; Elliott and Benjamin, 1989).

To measure the temporal parameters of the fictive feeding rhythm an interface to a microcomputer was constructed (Andrew, 1989). The clock in the interface was used to time the occurrences of action potentials in the patterned activity recorded from the isolated CNS. From these data, the durations of the motoneuronal bursts and of the interburst interval were determined. Comparison of the activity in pairs of cells was used to determine the duration of each phase (N1, N2 and N3) of the feeding rhythm. It will be shown that the duration of the rasp (N2) phase remains constant, however fast the rate of fictive feeding. In spontaneous rhythms (and in those driven by stimulating one N1 cell), over 90 % of the changes in cycle period are due to changes in the N3 (swallowing) phase. This is not true of SO-driven rhythms, where both N1 (protraction) and N3 phases change in duration.

Finally, as a way of testing the adequacy of the sequential model of the feeding system described above, the predictions of the model can be compared with the results of this temporal analysis. The results can be explained by the known connections and properties of the feeding interneurones.

Materials and methods

Snails

Pond snails, *Lymnaea stagnalis* (L.), were obtained from Blades Biological (Kent). As described recently (Elliott and Benjamin, 1989), they were kept in standard snail water and fed lettuce frequently. Selected snails were starved for 24 h, and then given lettuce. The first snail to crawl onto the lettuce and begin feeding (normally within 10 min) was selected for immediate dissection. This resulted in 'fictive feeding' in 80 % of preparations. For this series of experiments, 25 preparations were made and the results presented below were selected from 15 of these preparations in which the rhythmic sequence of N1, N2 and N3 synaptic activity was continuous, as judged by the synaptic inputs to the identified motoneurones.

Intracellular recording

Glass microelectrodes were pulled from 1 mm fibre-containing glass to a tip resistance of 10–30 MΩ when filled with 4 mol l^{-1} potassium acetate. All recordings were from the CNS isolated with a short length of oesophagus in normal Hepes saline (Elliott and Benjamin, 1989). The sheath was softened with 0.1 % protease (Sigma XIV) for 2–5 min and the neuronal somata were impaled.

Electrical activity was tape-recorded digitally on video-tape and played back on a Gould TA550 chart recorder.

Recordings were made from cells in the feeding system identified either visually (motoneurones 3 and 8) or by comparison of their pattern of synaptic inputs (cells 5, 6, 7 and 10) with those described previously (Rose and Benjamin, 1981*a*). The SO and N1 interneurones were identified by their firing pattern and by their ability to drive the feeding rhythm when depolarised tonically.

Interfacing

In initial experiments, the times of the beginnings and ends of bursts were measured from chart recordings using a Grafbar digitiser. In subsequent experiments, tape recordings were played back into a set of band-pass filters. The filtered output was fed to comparators set to generate TTL pulses on each action potential. These pulses were used to set individual bits in a status register and to control the output latch of a 1MHz clock on a custom-made board in an IBM-compatible microcomputer. Times were read and the status register cleared using a polling routine written in Turbo Pascal. Details of the circuit and data collection routines are given in Andrew (1989).

Data were transferred to a VAX minicomputer and the firing rate, times of bursts and interburst intervals determined. Regression lines, correlation coefficents and other statistical tests and graphic output were obtained from the Minitab package, while graphic output was produced on Uniras.

Results

Identification of N1, N2 and N3 phases

In many isolated CNS preparations, the motoneurones in the *Lymnaea* buccal ganglia show rhythmic bursts of spontaneous fictive feeding. The records from the 7 and 8 cells in Fig. 1A show typical bursts of correlated synaptic inputs and spiking activity, from which the N1, N2 and N3 phases of the feeding cycle can be visually identified (see Rose and Benjamin, 1981*a*). In the N1 phase, the 7 cell fires rapidly and the 8 cell is inhibited; in the N2 phase both cells are inhibited, whereas in the N3 phase both cells fire, but the 7 cell only reaches threshold slowly. In another preparation (Fig. 1B), rhythmic activity was induced by stimulating a modulatory interneurone, the SO. The 8 cell shows the same firing pattern as in the spontaneous rhythm (it only fires in the N3 phase), but the SO is active in both the N1 and part of the N3 phases.

The recordings in this study were from the SO and N1 interneurones and from buccal motoneurones known as 3, 5, 6, 7, 8 and 10 cells. Fig. 1C summarises their firing patterns during fictive feeding. In each cycle, the N1 neurones fire at a gradually increasing rate throughout the N1 phase. During this time the 3, 5 and 8 cells are inhibited, while the 6 and 7 cells fire. Most 10 cells show a gradual depolarisation (shaded triangle); a few may spike weakly. In the N2 phase only the 3 and 10 cells fire: all the other cells are silent. In the last (N3) phase of the rhythm,

the 8 cells fire continuously, the 5 and 7 cells fire tonically after an initial inhibitory input and the 3 cell produces a barrage of EPSPs which may give rise to a few spikes, especially at the beginning of the phase. The firing pattern of the SO is shown as a shaded bar since it is normally silent during spontaneously recorded rhythms and in those elicited by depolarising an N1 cell. However, if the rhythm is driven by injecting steady depolarising current into the SO, it fires in the latter part of the N3 phase and throughout the N1 phase.

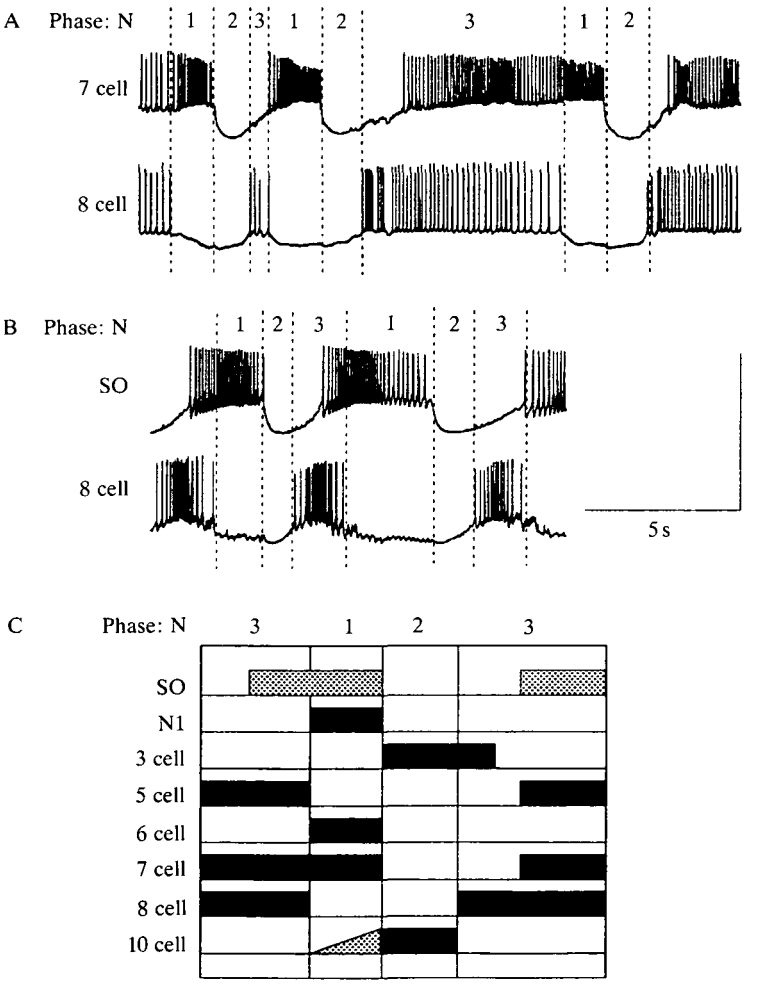

Fig. 1. Firing patterns of *Lymnaea stagnalis* buccal neurones during fictive feeding. (A) Recordings from two motoneurones (7 and 8 cells). (B) Recordings from an SO and an 8 cell. In A and B, the N1, N2 and N3 phases of activity have been indicated. (C) A summary diagram showing the firing patterns of selected neurones in the buccal ganglia during fictive feeding (solid bars). Only in SO-driven rhythms is the SO active in part of the cycle (shaded bar). Most 10 cells depolarise gradually in the N1 phase (shaded triangle). Scale bar: A, 7 cell 110 mV, 8 cell 120 mV; B, SO 90 mV, 8 cell 90 mV.

Although the phases of interneuronal activity are identified visually in Fig. 1A,B, the timing of the action potentials recorded from selected pairs of motoneurones can be sufficient to identify the times at which the three phases of interneuronal activity start and finish in each cycle of fictive feeding. For example, consider the recordings of the 7 and 8 cells shown in Fig. 1A. TTL pulses are produced from each action potential and are fed to a microcomputer where a 1MHz clock is used to provide two tables of the times of action potentials. Since the 8 cell stops firing at the start of the N1 phase, a simple search of the table of 8 cell action potential times for interburst intervals (always at least 1.2 s) provides an easy method for identifying the start of each feeding cycle. Within each cycle the beginning of the N2 phase can be determined from the time of the end of the 7 cell burst and the beginning of the N3 phase from the time of the first 8 cell spike. Similarly, for the record shown in Fig. 1B, the end of each 8 cell burst marks the beginning of the N1 phase, the end of the SO burst marks the start of the N2 phase and the first 8 cell spike marks the beginning of the N3 phase. Other pairs of cells whose action potentials suffice to identify the three phases of neural activity include the 5 and 8 cells, the 6 and 10 cells and the 7 and 10 cells.

Analysis of spontaneous fictive feeding

The feeding rate

When starved snails are given lettuce just before the experiment, rhythmic fictive feeding is seen in most preparations. In this spontaneous fictive feeding activity, the durations of the cycles of the rhythm vary from 2.5 to over 25 s (corresponding to feeding rates of 0.4 to less than 0.04 Hz). Sometimes the feeding rate drops even lower, but in such cases the feeding motoneurones generally show quiescent periods with no synaptic inputs from the pattern-generating (or other) interneurones. Fig. 2A is a time series plot, showing that the feeding rate (y-axis) varies greatly, even between successive cycles: there is no evidence for gradual changes from cycle to cycle. Fig. 2C shows a histogram of the cycle periods in a second preparation with a mean of 6.8 s and variance of $29s^2$. One possible model of the spontaneous feeding system would be that successive cycles occur with a constant probability, irrespective of the time since the beginning of the last cycle. In this case the cycle periods would follow the Poisson distribution with the same mean; this is also plotted in Fig. 2C. It is clear that the expected Poisson distribution has a much smaller variance and so this model must be rejected. The same result was found for each of the three preparations for which Poisson distributions were calculated. In three further preparations, the mean was significantly less ($P<0.02$) than the variance, showing that departures from the Poisson expectation occur reliably. Other possibilities that can be rejected are models in which the successive cycle periods are strongly correlated with each other. Six preparations were analysed by plotting the feeding rate in each cycle (1/cycle period) against that in the next one. In the case shown in Fig. 2B the slope of the regression line is 0.153. This confirms that the lengths of successive feeding

cycles are not strongly correlated. In none of the other five preparations was the slope of the regression significantly different from zero (range −0.075 to 0.12, $P>0.09$ in each case). In summary, the feeding rate (1/ cycle period) of the next cycle will be between 0.01 and 0.45 Hz, irrespective of the duration of the present cycle.

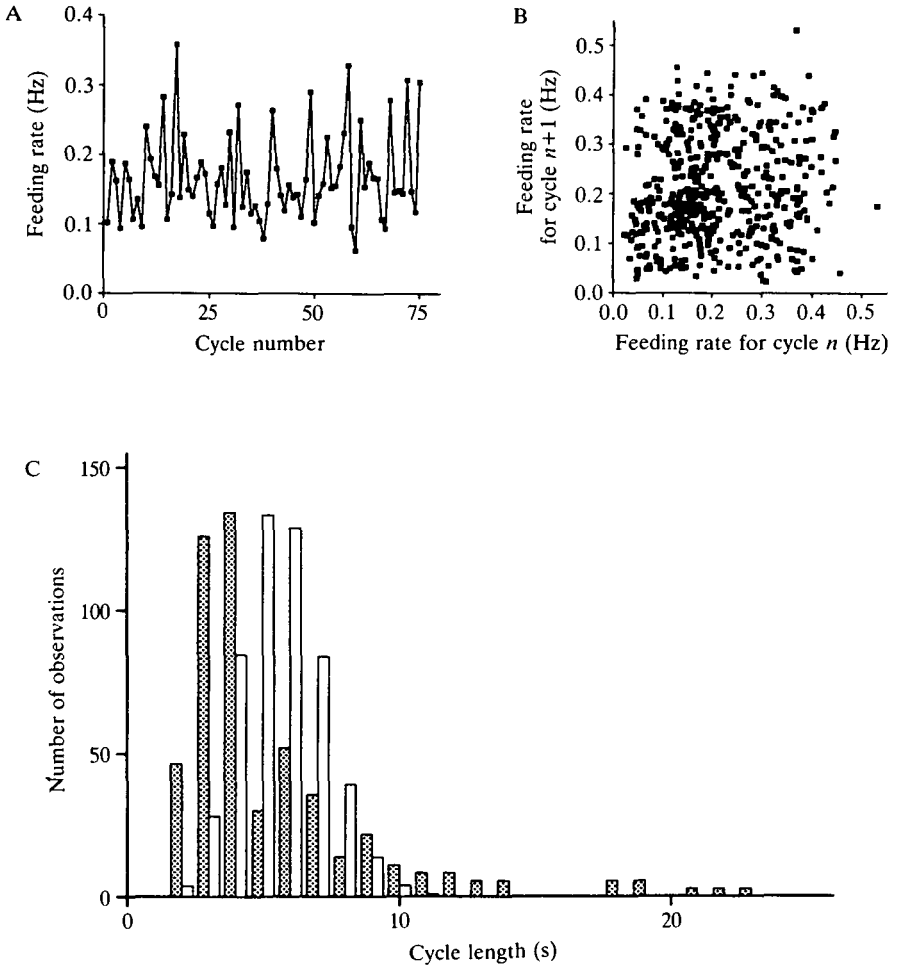

Fig. 2. The duration of spontaneous feeding cycles is 'random'. (A) A time series plot of the feeding rate (1/cycle period) in 75 successive cycles: sometimes fast and slow cycles alternate; at other times they occur together. (B) A diagram correlating the feeding rate in one cycle (x-axis) with that in the next cycle (y-axis) for 520 successive cycles of spontaneous fictive feeding. Note that the correlation is very weak, $r=0.153$. (C) A histogram of the distribution of the 520 cycle periods in the same preparation as B. The shaded bars show the observed frequencies (the 23 observations over 25 s have been excluded) and the open bars show the expected Poisson distribution for the same mean cycle period (6.8 s). Note the marked differences: there are many more fast and many more slow cycles than expected.

The neuronal firing rate

The firing rates of the motoneurones active in the N1, N2 and N3 phases were measured as an index of the synaptic input from the interneurones. The three motoneurones shown in Fig. 3A-C (7, 10 and 8 cells) were chosen as neurones active in the three phases of the fictive feeding rhythm and their firing rates are plotted as a function of the feeding rate. For motoneurones active in the N1 and N3 phases, the firing rate increases gradually as the feeding rate increases (Fig. 3A,C, slopes of 14.9 and 13.8, respectively, $P<0.001$ in both cases). This result has been found for each N1 and N3 phase motoneurone examined ($N=9$), but the slope of the regression is different in each preparation.

However, this result does not hold for the cells active in the N2 phase, where the motoneuronal firing rate does not increase with feeding rate but remains constant.

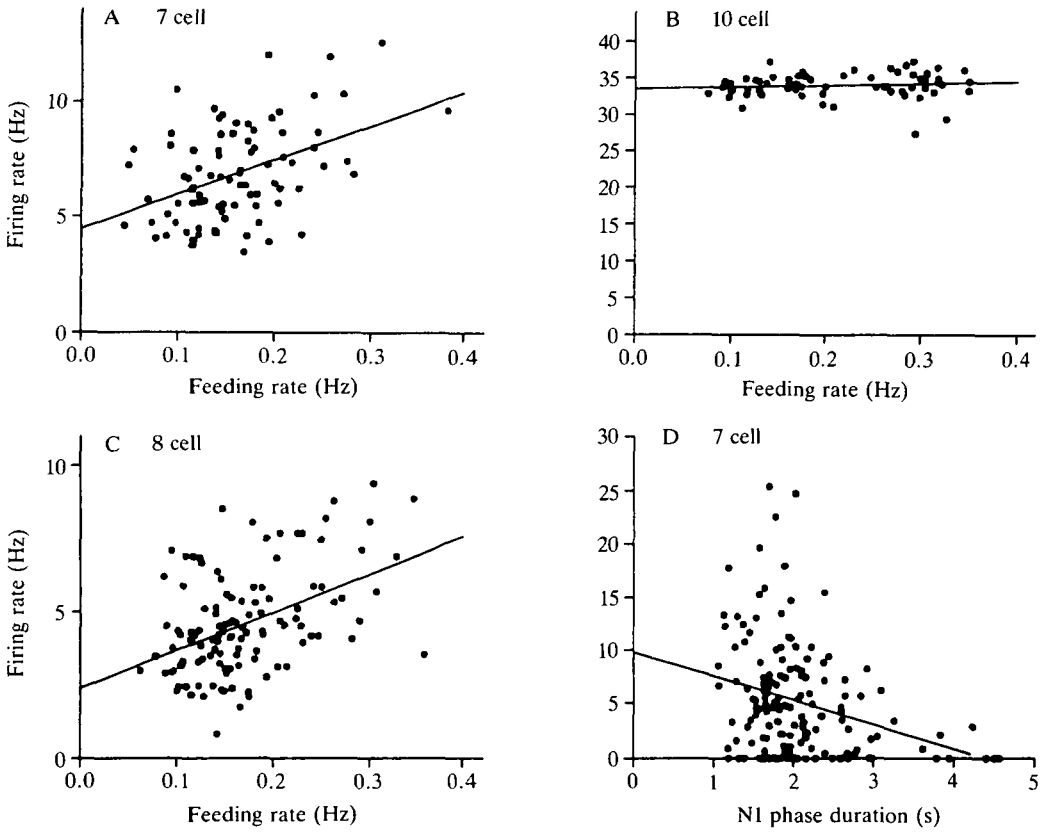

Fig. 3. The firing rates of motoneurones during (A) the N1, (B) the N2 and (C) the N3 phases of spontaneous fictive feeding as a function of the feeding rate. The firing rates of the motoneurones active in the N1 and the N3 phases but *not* the N2 phase are correlated with feeding rate. (Although the 7 cell fires in the N1 and N3 phases, its firing rate was only measured in the N1 phase; activity in the N3 phase was ignored). (D) A plot of the 7 cell firing rate (during the N1 phase) against the duration of the N1 phase. The motoneuronal firing rate is slower in long N1 phases.

The 10 cell is an example of such a cell, it fires solely in the N2 phase and maintains a steady firing rate, irrespective of feeding rate. In the example shown in Fig. 3B the firing rate is 34.0±1.7 Hz (mean±S.D., N=55); the slope of the regression between firing rate and feeding rate is 2.46 (much smaller than the slopes of the N1 and N3 relationships) and the associated correlation coefficient is not significant (r=0.118, P>0.3). This result has been found for three 10 cells. The other cell in this study that fires partly in the N2 phase is the 3 cell and we have confirmed in two preparations that its N2 phase firing rate is also uncorrelated with feeding rate.

Detailed analysis of the 7 cell firing pattern shows that its firing rate in the N1 phase decreases as the N1 phase gets longer (Fig. 3D, P<0.001). Since the 7 cell shows no adaptation of spike frequency with current injection (C. J. H. Elliott, personal observation), the most likely explanation for this is that the higher firing rates result from more excitatory synaptic input from the N1 interneurones. This implies that higher N1 firing rates should be associated with short N1 phases. (So far, this has been directly confirmed by analysis of the bursts of activity recorded from one N1 interneurone.)

Changes in the phase duration

If the feeding rate is so variable, in which phase (N1, N2 or N3) does any change occur? Figs 4 and 5 examine this question, showing results from the same preparation plotted in two different ways. In Fig. 4, the proportion of the cycle devoted to each phase of neuronal activity is plotted against feeding rate. As feeding gets faster, an increasing proportion of each cycle is occupied by N2 activity (Fig. 4B). With a slow feeding rate of 0.1 Hz, the N2 phase lasts for about 10% of the cycle, but it lasts for nearly 50% of the fastest (0.4 Hz) cycles recorded. A smaller increase is seen in the proportion of time occupied by the N1 phase (Fig. 4A). In contrast, the length of the N3 phase declines as the feeding rate increases: from 80% at 0.1 Hz to 20% at 0.4 Hz (Fig. 4C). These results show that, as the feeding rate increases, each phase does not account for a constant

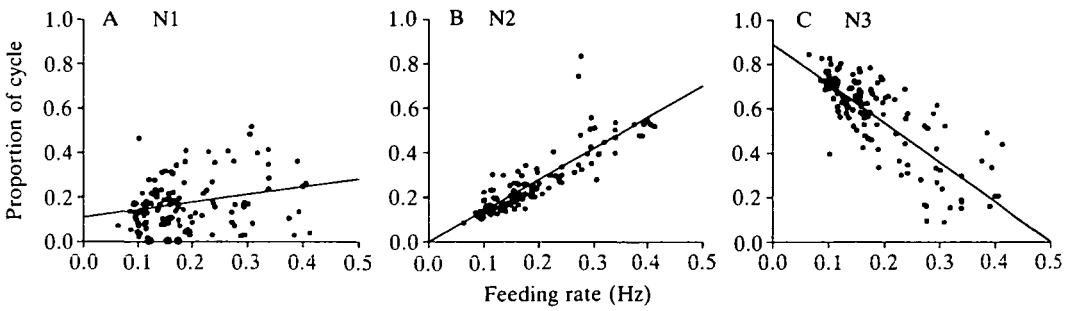

Fig. 4. The proportion of the fictive feeding cycle spent in (A) the N1, (B) the N2 and (C) the N3 phases plotted against feeding rate. Records are from 126 cycles of spontaneous feeding activity. Note that the proportion of the cycle spent in the N2 phase increases whereas the proportion spent in the N3 phase decreases as the feeding rate gets faster.

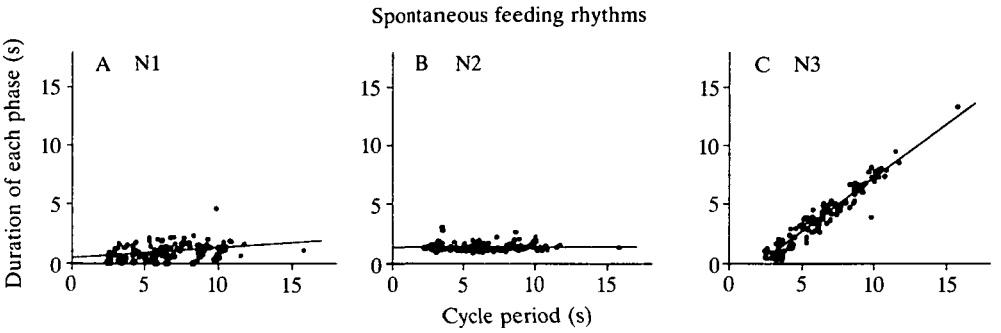

Fig. 5. The duration of the fictive feeding cycle spent in (A) the N1, (B) the N2 and (C) the N3 phases as a function of cycle period. Analysis of the same 126 spontaneous cycles as in Fig. 4; note that the horizontal axis of each part of Fig. 5 is the reciprocal of the corresponding frame in Fig. 4. The N2 phase has a fixed duration, whereas the N3 duration is proportional to cycle period, with a least-squares slope of 0.91.

proportion of each cycle. In other words, as the feeding rate increases, the changes are not distributed equally throughout the three types of N-cell in the network.

Another analysis of the same spontaneous fictive feeding rhythm is shown in Fig. 5. This time the durations of N1, N2 and N3 activity are plotted against the cycle period. Note that the N2 duration remains virtually constant (mean 1.37 s), irrespective of cycle period (the slope of the regression line is 0.002) and that there is only a small increase in the N1 duration (the slope is 0.085). However, the N3 result is very different: the duration of the N3 phase increases rapidly with cycle period, accounting for almost all of the variation, with the slope of the regression line being 0.91 in this experiment. The change in the duration of the N3 phase (and constancy of the N1 and N2 phases) may be seen in Fig. 1A, where the two successive N3 phases illustrated last for 0.5 and 5.5 s, respectively.

The average results from the four preparations analysed in this way are shown in Fig. 6 (open bars). In each case the duration of the N3 phase varies with cycle period (slope=0.92±0.015, mean±S.E.) while the lengths of the N1 and N2 phases are constant (the probability that the slope of the regression is greater than zero is not significant).

Analysis of evoked fictive feeding

Fictive feeding can be evoked in most quiescent preparations by stimulating either an N1 or an SO interneurone with steady depolarising current. In either case the normal sequence of interneuronal activity (N1→N2→N3→N1...) is recorded and this leads to the same sequence of motoneuronal firing activity. Increases in the stimulating current increase the firing rate of the driving cell and the feeding rate (Rose and Benjamin, 1981*a*). In preparations that show spontaneous fictive feeding, SO or N1 stimulation steps up the feeding rate.

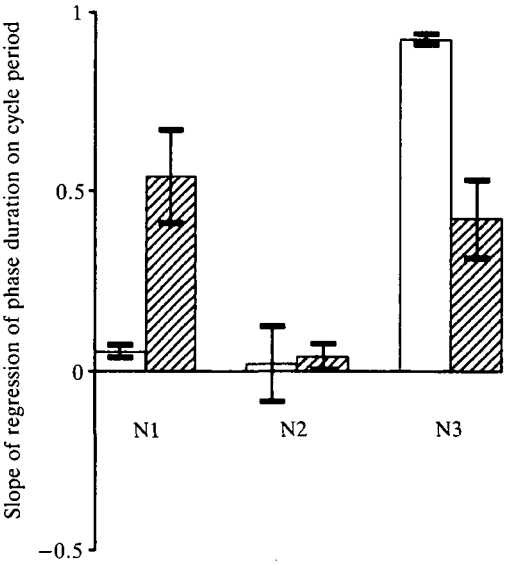

Fig. 6. A summary of the localisation of the variation in cycle period. Regression lines of the relationship between cycle period and the duration of the N1, N2 and N3 phases were calculated for each preparation. This figure plots the mean (±S.E.) slope of the regression lines. Four spontaneous rhythms (open bars) and four SO-driven rhythms (shaded bars) were analysed. In spontaneous rhythms the alterations in N3 phase duration account for 92% of the changes in cycle period. In SO-driven rhythms the durations of N1 and N3 phases both change significantly with cycle period (Mann–Whitney tests, $P<0.05$ in both cases). The duration of the N2 phase is never correlated with cycle period.

Effects of N1 stimulation

Stimulation of an N1 cell results in an acceleration of the rate of spontaneous fictive feeding or, in inactive preparations, leads to rhythmic activity. Fig. 7 shows the results of one experiment in which different strengths of current were used to obtain different feeding rates. The N1 and N2 durations were nearly constant with slopes of 0.10 and 0.02, respectively (both not significant). As with the spontaneous rhythms, virtually all the variation can be accounted for by alterations in the N3 phase of the rhythm. In this case the slope of the regression is 0.87. In cycles of less than 5 s duration, the entire time is taken up by activity in the N1 or N2 phases and any N3 input is extremely short and weak.

Effects of SO stimulation

When the SO is weakly stimulated, it fires tonically and slowly. The intervals between action potentials are too long for the SO→N1 synapse to facilitate and no activity is recorded in the premotor N-cells. With stronger stimulation, the full sequence of N1, N2 and N3 activity is seen and the cycle rate depends on the strength of the stimulus. The durations of the N1, N2 and N3 phases are plotted

against the cycle period in Fig. 8, which shows that the durations of the N1 and N3 phases both increase with cycle period while the N2 duration remains constant. This result is also seen in the record illustated in Fig. 1B (note the much longer duration of the N1 phase in the second of the two cycles shown). Regression

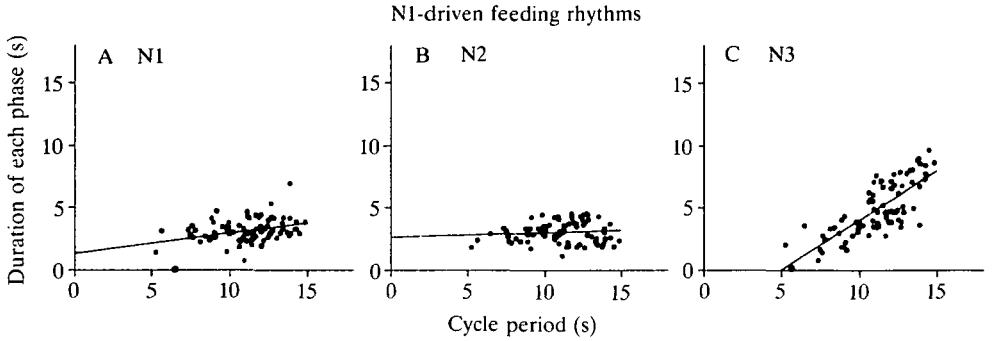

Fig. 7. Analysis of N1-driven fictive feeding. The duration of the feeding cycle spent in (A) the N1, (B) the N2 and (C) the N3 phases as a function of cycle period. Records are from 95 cycles. The N2 phase has a fixed duration, whereas the N3 duration is proportional to cycle period. Note that the results displayed in this figure very closely resemble those in Fig. 5, which is plotted on the same scale.

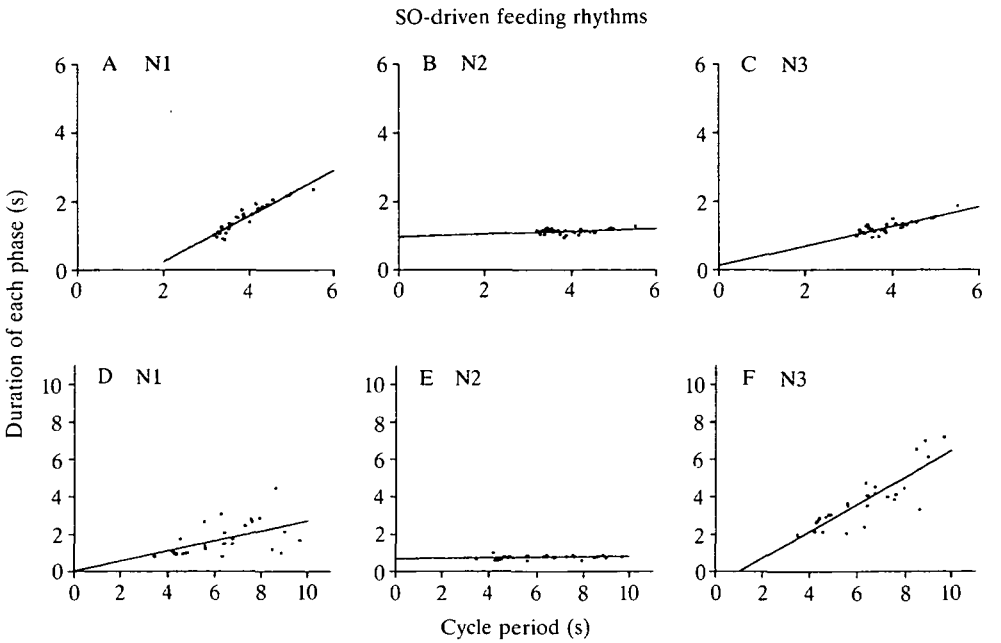

Fig. 8. Analysis of SO-driven fictive feeding in two preparations. (A–C) Records from 45 cycles. The duration of the feeding cycle spent in (A) the N1, (B) the N2 and (C) the N3 phases is plotted as a function of cycle period. (D–F) Corresponding plots using records from 33 cycles in another preparation. The N2 phase has a fixed duration, whereas the N1 and N3 durations both increase with cycle period. Compare Figs 5 and 7 from spontaneous and N1-driven rhythms.

analysis of the data in Fig. 8A shows that the slope of the relationship between N1 duration and the cycle period is 0.78 and, in Fig. 8C, that the slope for N3 regression is 0.24. The N2 slope in this preparation is 0.02. There is a significant positive correlation between N1 duration and the cycle period of the four preparations examined quantitatively ($P<0.01$ for each): the mean results are shown in Fig. 6.

In Fig. 8A, it might appear that the slope of the relationship between N1 duration and cycle period is beginning to decline with longer cycles. To investigate this, a preparation with very slow SO rhythms and with cycle periods up to 10 s was selected for analysis (Fig. 8D–F). In this preparation, the N1 phase continues to increase in duration as the cycle period increases up to the 10 s limit. However, the slope of the regression of N1 duration on cycle period (0.27) is less than that in Fig. 8A, where the slowest cycle period was 6 s. (None of the spontaneous or N1-driven rhythms show slopes exceeding 0.1, even when the data are restricted to cycle periods of less than 6 s.)

In summary, with SO stimulation the rhythm is quantitatively different from that of spontaneous rhythms, since in the SO-driven rhythms the N1 slope is significantly greater than zero. Also, the N3 slope is much less than that in the spontaneous rhythms ($P=0.030$). Nonetheless, in both cases, the N2 duration remains constant.

Discussion

The aim of these experiments is to describe the temporal patterning of the feeding rhythm in *Lymnaea stagnalis*. In particular, the results will be analysed to identify variant or consistent parts of the three-phase rhythm (N1, N2 and N3) and will be related to the sequential model of the snail feeding rhythm which was derived from studies of the synaptic connections and endogenous membrane properties (Rose and Benjamin, 1981*a*,*b*; Elliott and Benjamin, 1985*a*,*b*).

Temporal analysis of fictive feeding

Spontaneous fictive feeding in the isolated CNS of *L. stagnalis* occurs randomly in the sense that the duration of the next cycle is not well predicted by the length of the present cycle (Fig. 2B). However, the data do not support a model in which the start of the cycles occurs with a constant probability per unit time; such a model predicts a Poisson distribution of cycle times and the data do not fit this distribution well (Fig. 2C). Altering the starting point of the Poisson model (e.g. for the probability to begin only at the end of the N2 phase rather than at the start of the cycle) does not improve the goodness of fit. It would appear that the probability of starting the next cycle is high during the first 1–3 s of an N3 phase and declines thereafter (Fig. 2C).

The firing rates of the motoneurones active in the N1 and N3 phases increase with the feeding rate, but those motoneurones active in the N2 phase fire at a constant rate irrespective of the feeding rate (Fig. 3A–C). Since the firing rates of

the 5, 7, 8 and 10 cells do not adapt rapidly to injected currents (C. J. H. Elliott, personal observation), their firing rates are likely to reflect the amount of transmitter released by the interneurones. We suggest, therefore, that the firing rate of the N2 interneurones is likely to be independent of feeding rate, while the N1 and N3 interneurones will fire more rapidly with faster feeding.

The results from spontaneous feeding rhythms demonstrate clearly that nearly all (just over 90%) of the changes in cycle period arise from alterations in the duration of the N3 phase (Figs 5, 6). This is also the case in those rhythms evoked by N1 stimulation (Fig. 7). However, in all circumstances, the N2 phase appears to be fixed in length. This analysis means that the system of interneurones involved in feeding must be organised so that, once N1 activity has begun, the N1 and N2 phases will occur with more or less constant duration, and all changes take place in the N3 phase. This rule is not followed by SO-driven rhythms, where changes in the N1 duration are as large as the N3 changes (Figs 6, 8).

Although no data are available from intact *Lymnaea stagnalis*, recordings from semi-intact preparations indicate that the N2 phase duration is the least variable (Rose and Benjamin, 1979), which agrees with the observations reported here. Furthermore, the variation in N1 duration seen in many of the recordings that Rose and Benjamin made using sucrose application is not unexpected, since sucrose excites the SO (Kemenes *et al.* 1986). However, comparison with genuine snail feeding behaviour must await quantitative analysis of fine-wire recordings from freely moving snails.

It is really quite surprising that the N2 phase of the snail feeding cycle should be so invariant, because this phase of interneuronal activity corresponds to the behavioural activity of rasping, during which the radula is scraped over the food, e.g. lettuce or algae (Rose and Benjamin, 1979). This would be the stage at which sensory feedback might be expected to have the most dominant role in the behaviour (Benjamin *et al.* 1985), and so it might be expected that the behaviour pattern would be most flexible at this phase of the rhythm. Even though these experiments were on the isolated CNS, it might still be expected that the N2 (rasping) phase would show the greatest variability in duration and motoneuronal firing rate; if sensory input is to be effective it seems odd that it should have to compete with a fixed pattern of central programming.

The feeding rhythm can be described approximately as a three-stroke relaxation oscillator. Relaxation oscillators (see Murray, 1989, for details) are common in biological systems, including those for insect walking and breathing (Pearson, 1972; Lewis *et al.* 1973). In a normal two-stroke relaxation oscillator, the duration of one stroke is variable and that of the other is fixed. In general, the variable part of biological oscillators tends to be the power stroke, e.g. in cockroach walking (Pearson, 1972), but in the case of feeding in *Lymnaea stagnalis* the opposite seems to be true, since the N1 and N2 phases, which move the radula, are the most fixed.

Temporal predictions of the interneuronal model

The synaptic interactions of the modulatory interneurones (CGCs and SO) and

pattern-generating interneurones (N1, N2, N3) recorded by Elliott and Benjamin (1985*a*,*b*) are shown in Fig. 9. The model proceeds as follows. To start the rhythmic activity, a stimulating current is injected into an N1 cell. The N1 activity has two effects: first, it inhibits the normal tonic activity of the N3 neurones; second, it excites and gradually depolarises the N2 cells. When the N2 cells reach threshold, they fire a burst of action potentials and inhibit the N1 cells, thus switching from the N1 to the N2 phase. This model would predict that stimulating an N1 cell more strongly would result in a shorter N1 phase. This is in agreement with the results presented in this paper: there is a significant negative correlation between the duration of the N1 phase and the firing rate of interneurones and motoneurones active in this phase (Fig. 3D).

Alternative models (including that suggested by Rose and Benjamin, 1981*b*) suggest that the N1 and N2 neurones should be connected by reciprocal inhibition. In this case, a high frequency of N1 firing would be expected to strengthen the inhibitory input to the N2 cells and so prolong the N1 bursts. However, our evidence suggests that this model can be rejected, since high N1 firing rates are associated with shorter bursts (Fig. 3D).

Returning to the description of activity in the model shown in Fig. 9, the next step is that the N2 neurones fire briefly and inhibit the N3 interneurones (as well as the N1 cells). Once activity in the N2 neurones is triggered, a sustained plateau

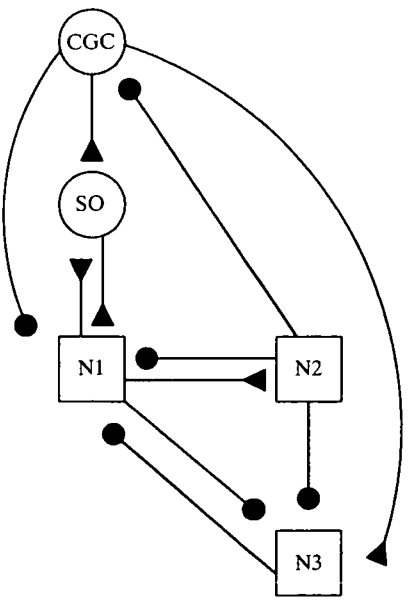

Fig. 9. Synaptic model of the feeding system of *Lymnaea,* based on Elliott and Benjamin (1985*a*,*b*) and Benjamin *et al.* (1981). Excitatory connections are shown as filled triangles; filled circles are inhibitory connections. The circles represent unique (SO) or paired (CGC) identified neurones; squares represent populations of neurones (N1, N2 and N3). The connections within the buccal ganglia (SO, N1, N2 and N3) are thought to be monosynaptic (Elliott and Benjamin, 1985*a*,*b*).

potential is initiated, which is not terminated by any known synaptic inputs. The fact that this potential terminates itself suggests that it is best classified along with the driver potentials recorded in crustacean cardiac ganglia (Tazaki and Cooke, 1979; for overviews, see Cooke, 1988; Hartline *et al.* 1988). Such a fixed neuronal event would explain the constant duration of the N2 phase (Figs 5, 6) and firing frequency (Fig. 3B).

Once the N1 and N2 inhibition of the N3 cells has died away, the N3 cells depolarise and fire as a result of a combination of post-inhibitory rebound (PIR) and excitatory input from the tonically active CGCs in the cerebral ganglia (Benjamin and Elliott, 1989). The PIR and CGC input together bring about the N3 phase of the feeding rhythm. The strong effect of the PIR explains why the N3 phase rarely lasts less than 1 s; the tonic effects of the CGCs (excitatory to N3 neurones, inhibitory to N1 neurones) can explain the frequently long N3 phase.

We may suppose that the rapidly firing N3 neurones would lead to a high motoneuronal firing rate and would strongly inhibit the N1 interneurones, so prolonging the N3 phase and hence the cycle period. In other words, high firing rates in the N3 phase should be correlated with long cycle periods. This is not found; high firing rates of the motoneurones in the N3 phase are associated with high feeding rates (Fig. 3C) and short N3 phases (Fig. 5). Thus, it would appear that direct modulation of the motoneuronal firing rate, by the CGCs for example (McCrohan and Benjamin, 1980), is more important than inputs from the pattern-generating neurones in the N3 phase. This provides direct evidence for the independent modulation of intensity and frequency of the rhythm. The end of the N3 phase marks the start of the next feeding cycle. The failure of the frequency distribution of cycle periods to follow the Poisson distribution (Fig. 2) may also arise from changes in N3 activity brought about by variation in CGC input.

Different feeding rhythms were driven by stimulating the SO cell (Fig. 8). According to the Elliott and Benjamin (1985*b*) model, the main effect of the SO is to excite the N1 interneurones, while the N1 neurones themselves reciprocally excite the SO. When the SO firing rate is sufficient to lead to facilitating SO→N1 synaptic potentials, rhythmic activity begins. With stronger SO stimulation, the reciprocal excitatory connections come into play more quickly and so cause a more rapid build up of N1 activity. Thus, the N1 neurones will excite the N2 cells to threshold sooner, leading to a shorter N1 phase. In this way the reduction of N1 duration with decreased cycle period in SO-driven rhythms can be explained (Figs 6, 8). This represents a difference from the N1-driven and spontaneous rhythms, where the build-up of activity in the N1 cells is thought to depend on their ability to burst endogenously (Elliott and Benjamin, 1985*a*).

In conclusion, quantitative temporal analysis provides a framework within which any future explanation of the origin of the feeding rhythm must fit. The proposed model of the connections between the pattern-generating N-cells can explain the differences in the duration of the N1 phase in the spontaneous and SO-driven rhythms, the constancy of the N2 phase in duration and motoneuronal firing rate and the correlation between N1 phase firing rate and N1 duration

However, problems appear in the N3 phase, where it seems that the influence of other modulatory neurones (e.g. the CGCs) are more important than the N-cell inputs.

We should like to thank the SERC (UK) for their support and Dr G. Kemenes for reading the manuscript.

References

ANDREW, T. (1989). Timing activity in snail neurons during feeding. MSc thesis, University of York.

BENJAMIN, P. R. AND ELLIOTT, C. J. H. (1989). Snail feeding oscillator: the central pattern generator and its control by modulatory interneurons. In *Neuronal and Cellular Oscillators* (ed. J. W. Jacklet), pp. 173–214. New York, Basel: Marcel Dekker.

BENJAMIN, P. R., ELLIOTT, C. J. H. AND FERGUSON, G. P. (1985). Neural network analysis in the snail brain. In *Model Neural Networks And Behavior* (ed. A. I. Selverston), pp. 87–103. New York: Plenum press

BENJAMIN, P. R., MCCROHAN, C. R. AND ROSE, R. M. (1981). Higher order interneurones which initiate and modulate feeding in the pond snail *Lymnaea stagnalis*. In *Neurobiology of Invertebrates, Mechanisms of integration* (ed. J. Sálanki), pp. 171–200. Oxford: Pergamon Press.

BENJAMIN, P. R. AND ROSE, R. M. (1979). Central generation of bursting in the feeding system of the snail, *Lymnaea stagnalis*. *J. exp. Biol.* **80**, 93–118.

COOKE, I. M. (1988). Studies on the crustacean cardiac ganglion. *Comp. Biochem. Physiol.* **91**C, 205–218.

DAWKINS, M. (1974). Behavioural analysis of coordinated feeding movements in the gastropod *Lymnaea stagnalis*. *J. comp. Physiol.* **92**, 255–271.

ELLIOTT, C. J. H. AND BENJAMIN, P. R. (1985*a*). Interactions of pattern generating interneurons controlling feeding in *Lymnaea stagnalis*. *J. Neurophysiol.* **54**, 1396–1411.

ELLIOTT, C. J. H. AND BENJAMIN, P. R. (1985*b*). Interactions of the slow oscillator interneuron with feeding pattern generating interneurons in *Lymnaea stagnalis*. *J. Neurophysiol.* **54**, 1412–1421.

ELLIOTT, C. J. H. AND BENJAMIN, P. R. (1989). Esophageal mechanoreceptors in the feeding system of the pond snail *Lymnaea stagnalis*. *J. Neurophysiol.* **61**, 727–736.

HARTLINE, D. K., RUSSELL, D. F., RAPER, J. A. AND GRAUBARD, K. (1988). Special cellular and synaptic mechanisms in motor pattern generators. *Comp. Biochem. Physiol.* **91**C, 115–131.

KEMENES, G., ELLIOTT, C. J. H. AND BENJAMIN, P. R. (1986). Chemical and tactile inputs to the *Lymnaea* feeding system: effects on behaviour and neural circuitry. *J. exp. Biol.* **122**, 113–137.

LEWIS, G. W., MILLER, P. L. AND MILLS, P. S. (1973). Neuromuscular mechanisms of abdominal pumping in the locust. *J. exp. Biol.* **59**, 149–168.

MCCROHAN, C. R. AND AUDESIRK, T. E. (1987). Initiation, maintenance and modification of patterned buccal motor output by the cerebral giant cells of *Lymnaea stagnalis*. *Comp. Biochem. Physiol.* **87**A, 969–977.

MCCROHAN, C. R. AND BENJAMIN, P. R. (1980). Synaptic relationships of the cerebral giant cells with motoneurones in the feeding system of *Lymnaea stagnalis*. *J. exp. Biol.* **85**, 169–186.

MURRAY, J. D. (1989). *Mathematical Biology*. Berlin, Heidelberg, New York: Springer-Verlag.

PEARSON, K. G. (1972). Central programming and reflex control in the cockroach *Periplaneta americana*. *J exp. Biol.* **56**, 173–193.

ROSE, R. M. AND BENJAMIN, P. R. (1979). The relationship of the central motor pattern to the feeding cycle of *Lymnaea stagnalis*. *J. exp. Biol.* **80**, 137–163.

ROSE, R. M. AND BENJAMIN, P. R. (1981*a*). Interneuronal control of feeding in the pond snail, *Lymnaea stagnalis*. I. Initiation of feeding cycles by a single buccal interneurone. *J. exp. Biol.* **92**, 187–201.

ROSE, R. M. AND BENJAMIN, P. R. (1981*b*). Interneuronal control of feeding in the pond snail,

Lymnaea stagnalis. II. The interneuronal mechanism generating feeding cycles. *J. exp. Biol.* **92**, 203–228.

TAZAKI, K. AND COOKE, I. M. (1979). Isolation and characterisation of slow, depolarising responses of cardiac ganglion neurons in the crab, *Portunus sanguinolentus J. Neurophysiol.* **42**, 1000–1021.

TUERSLEY, M. D. AND MCCROHAN, C. R. (1988). Serotonergic modulation of patterned motor output in *Lymnaea stagnalis*. *J. exp. Biol.* **135**, 473–486.